Micro-buried spiral zone plate in a lithium niobate crystal

Zhen-Nan Tian, Jian-Guan Hua, Juan Hao, Yan-Hao Yu, Qi-Dai Chen, and Hong-Bo Sun

Citation: Appl. Phys. Lett. **110**, 041102 (2017); doi: 10.1063/1.4974351
View online: http://dx.doi.org/10.1063/1.4974351
View Table of Contents: http://aip.scitation.org/toc/apl/110/4
Published by the American Institute of Physics

Micro-buried spiral zone plate in a lithium niobate crystal

Zhen-Nan Tian, Jian-Guan Hua, Juan Hao, Yan-Hao Yu, Qi-Dai Chen,[a] and Hong-Bo Sun
State Key Laboratory on Integrated Optoelectronics, College of Electronic Science and Engineering, Jilin University, 2699 Qianjin Street, Changchun 130012, People's Republic of China

(Received 7 November 2016; accepted 7 January 2017; published online 23 January 2017)

We present a micro-buried spiral zone plate (MBSZP) in the lithium niobate crystal fabricated with femtosecond laser direct writing technology. The microstructures of the MBSZP are buried under the surface of the crystal, which ensures the stability of the optical performance in various refractive index environments. The optical performances of imaging and focusing capabilities were demonstrated. In addition, the experiment showed good agreement with simulation results based on the optical wave propagation method. This novel optical element will have important applications in multistate information encoding, optical manipulation, quantum communication, and computation, especially in high integration, contact coupling, and variable refractive index environments. *Published by AIP Publishing*. [http://dx.doi.org/10.1063/1.4974351]

Optical phase singularities have been an enticing topic for both theoretical and applied research over the last couple of decades after their discovery by Allen *et al.* in 1992.[1] Optical vortices (OV), focused from a light wave with optical phase singularities, referring to the light beam carrying orbital angular momentum (OAM), have attracted great interest for their fascinating properties and potential applications.[2–5] OV beams have been widely applied in the manipulation of microscopic particles, an extraordinarily significant task in physics, chemistry, and biology.[6–8] Especially in the field of biology, their ability to transport and modify cells precisely without optical damage has led to clinical applications in areas such as *in vitro* fertilization.[9,10] As a new generation of light forces, OV beams not only trap and guide particles but also realize rotation and more complex trajectories.[11–13] In fact, they are leading a revolution in the fields of biology, physical chemistry, and soft condensed matter physics.[10]

Various methods have been proposed to generate OV beams, such as spiral phase plate,[14,15] computer-generated holograms,[16–18] cylindrical mode converter,[19] Q-plates,[20] metasurface,[21–23] and spatial light modulator.[24,25] The methods based on diffractive optical theory, light field modulation by phase delay, have been widely used for their light weight, small size, easy integration, and low cost. However, the diffractive units with microstructure to nanostructure size are exposed to the environment, where they can be easily broken and covered with impurities. Furthermore, the optical properties will change or even disappear entirely in environments with different refractive indices. In a special, extreme condition, the environment and the diffractive element have the same refractive index. The phase delay will disappear, thus removing the ability to modulate the light field. In addition, the conventional OV generators are bulky and hence restrict their employment in integrated optics. These restraints have inspired researchers to seek methods to reduce the size of OV generators.[26] In recent years, femtosecond laser direct writing technology (FsLDW), due to its characteristics of simplicity, flexibility, and high precision in material microstructuring, has been successfully employed to process various materials.[27–30] It offers novel approaches and ideas to solve the above problems.

In this work, we propose a novel micro-buried spiral zone plate (MBSZP) for generating microsized OV beams. The buried optical element was fabricated with femtosecond laser direct writing technology, which is an important and unique method for fabricating three-dimensional microstructures inside material owing to multi-photon absorption effect.[31–33] The MBSZP was buried inside of a lithium niobate crystal, whose surface has not been destroyed. It ensures that the MBSZP can be used in a variety of refractive index changing environments without obvious changes of the optical properties. The novel MBSZP will significantly improve the miniaturization and integration of OV generators, especially in different liquid environments and coupling interfaces at different media.

OV beams have a helical phase profile in their propagation direction, whose local pointing vector direction is different from the optical axis direction. In the plane perpendicular to the optical axis, the phase change of the light field can be described by $il\phi$, where l is the eigenvalue of the OAM or the so-called topological charge and ϕ is the azimuthal angle. A spiral zone plate (SZP) can work as an OV beam generator. It is equivalent to optically performing the radial Hilbert filtering operation and the imaging operation in a single step. The radial Hilbert phase function is given by

$$H_p(r,\phi) = \exp(ip\phi), \tag{1}$$

where p represents the topological charge, and r and ϕ are the polar coordinates. The Fresnel zone plate (FZP) phase function is given by

$$Fzp(r,\phi) = \exp(-i2\pi/\lambda f), \tag{2}$$

where λ is the wavelength and f is the focal length of the Fresnel zone plate. The SZP is obtained by multiplying the

[a]Author to whom correspondence should be addressed. Electronic mail: chenqd@jlu.edu.cn

radial Hilbert phase function with the FZP phase function and is given by

$$SZP_p(r,\phi) = H_p(r,\phi) * F_{zp}(r,\phi) = \exp(ip\phi - i2\pi/\lambda f). \tag{3}$$

The phase structure of formulas (1), (2), and (3) can modulate the light field with phase delay elements, which are shown in Figs. 1(a)–1(c), respectively. In Fig. 1(a), the phase change around center is 2π, which is decided by parameter p in formula (1). The focal length f and wavelength λ are 160 μm and 0.633 μm, respectively. The phase structure of SZP, the product of the radial Hilbert phase and the FZP phase, is shown in Fig. 1(c). Considering the processing accuracy and feasibility of production, the phase structure shown in Fig. 1(c) was two order quantized into the form of Fig. 1(d). There are only two kinds of phase values in the figure, 0 and π. The optical element can be realized by processing the dark red region with a phase value of π.

The buried optical element was fabricated with FsLDW, which is widely known as a high precision micro-machining technology. A laser source (Light-Conversion Pharos) was delivering less than 290-fs pulses of 1030-nm wavelength at a repetition rate of 200 kHz. A third harmonic generation system integrated in laser was used to get 343-nm laser light for improving machining accuracy and realizing two-photon-absorption at laser focus. In the z-cut lithium niobate crystal wafer without ion doping, femtosecond laser pulses were tightly focused through a high numerical aperture (NA = 1.35, 40×) objective lens and scanned by a two-galvano-mirror setup. Pulse energy was 0.45 μJ measured in front of the objective. The sample was fixed on a piezo stage with 1-nm precision (PI P-622ZCD), which controlled the scanning depth of the laser focus. The three-dimensional relative motion of the laser focus and the sample was realized by the cooperation of the piezo stage and the two-galvano-mirror setup. The whole process was completed at room temperature.

In order to reduce the influence of the change of the external environment on the optical properties, the SZP was processed under the surface of a lithium niobate crystal. The refractive index changed after laser scanning. Phase delay occurs when light passes through the scanned and unscanned regions. In this way, the incident light field is modulated to realize the desired optical function. Optical images of the MBSZP with topological charge of one are shown in Fig. 2. The diameter, height, and focal length are 80 μm, 15 μm, and 160 μm, respectively. The smallest out zone with a width of 0.8 μm can be observed clearly in Fig. 2(b). Four small right angles were fabricated on the crystal surface for comparing the buried properties of the MBSZP. Figs. 2(a) and 2(b) were taken at the surface and under the surface at a depth of 20 μm. In Fig. 2(a), the four black right angles surrounded the MBSZP are clearly seen, but the MBSZP is more difficult to be identified. However, under the surface at a depth of 20 μm, shown in Fig. 2(b), the MBSZP can be seen clearly with the right angles becoming blurred.

The refractive index of the environment has an important influence on the optical properties of diffractive elements. Here, the MBSZP were buried in the substrate materials, which can reduce the above effect and protect the micro size diffractive structures. The optical performances of imaging and focusing in different refractive index environments were evaluated by a microscope imaging system shown in Fig. 3, where an MBSZP with topological number of one was used. A letter "F," used as the imaging object, was fixed on a three-dimensional, movable sample stage and placed in front of the MBSZP, which was irradiated by a focused sodium lamp. An objective and a CCD camera were placed on the other side of the MBSZP and fixed on a movable stage. By adjusting the positions of the "F" and the objective, imaging results were detected. In the experiment, the imaging performance was tested in four different environments, air, water, $(CH_2OH)_2$, and cedar oil, whose refractive indices are 1, 1.33, 1.43, and 1.52, respectively [Figs. 3(a)–3(d)]. In the process of image acquisition, the relative position of the object, MBSZP, and

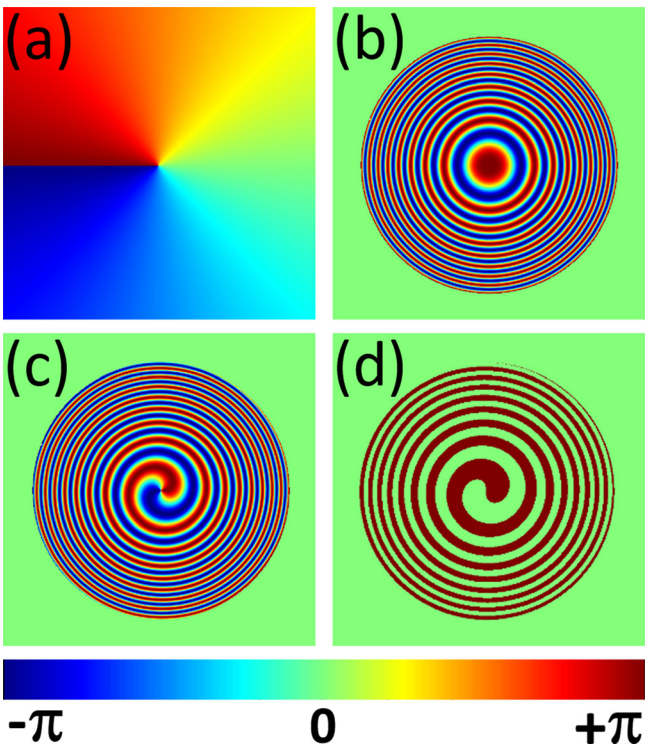

FIG. 1. Calculation process of two order SZP phase distribution. (a)–(c) The radial Hilbert phase structure, Fresnel zone plate phase structure, and spiral zone plate phase structure corresponding formulas (1)–(3), respectively. (d) Phase structure of the spiral zone plate after two order quantization.

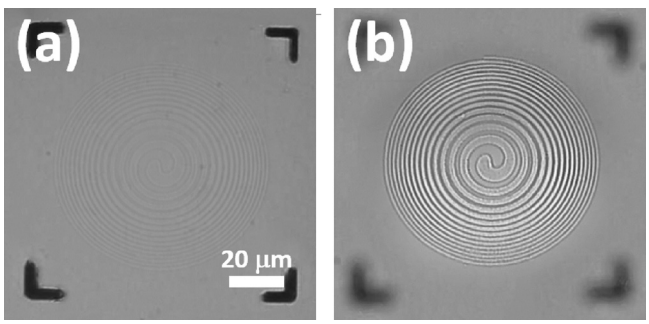

FIG. 2. Optical microscope images of the MBSZP. (a) Taken at the surface of sample. (b) Under the surface at a depth of 20 μm. Notice that the MBSZP and small right angles cannot be clearly imaged at the same time as they have different depths.

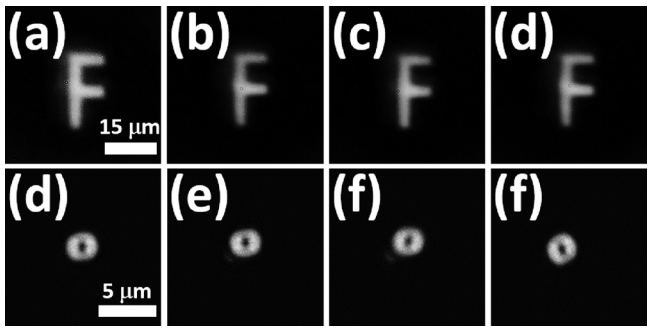

FIG. 3. Imaging and focusing properties demonstration in different environment. Imaging of the letter "F" in air (a), water (b), $(CH_2OH)_2$ (c), and cedar oil (d). The hollow rings at focal plane in air (e), water (f), $(CH_2OH)_2$ (g), and cedar oil (h). An MBSZP with topological number of one was used.

camera remains unchanged. The imaging quality of the MBSZP is independent of the different environments. This is because the diffractive structures were buried under the surface and the phase delay process was finished without the influence of the external environment.

A significant feature of the MBSZP, compared to a normal Fresnel zone plate, is the focusing property of light. When light passes through the MBSZP, a hollow light ring is obtained at the focal plane instead of a solid light spot. This is a unique and important property of OV beams. Compared with a solid light spot, the hollow light ring has a lower possibility of ablation, especially in the manipulation of biological tissue and cells. At present, particle manipulation is almost always performed in solution.[34,35] The refractive index of the solution has an important influence on the optical field. The MBSZP, buried under the surface of a crystal, does not directly contact the solution and can therefore circumvent the above problems. The focusing performances in environments with different refractive indices are shown in Fig. 3. For this experiment, the imaging object and sodium lamp were replaced with a collimated He-Ne laser. The hollow rings were obtained in the focal plane in air, water, $(CH_2OH)_2$, and cedar oil as shown in Figs. 3(e)–3(h), respectively. It can be seen from the images that there is no significant difference in size and brightness of hollow rings in different environments. The impact of the external environment has been suppressed.

When manipulating particles using vortex beams, the size of hollow ring is an important parameter, which determines the shear force strength. The size is decided by topological number of vortex beams. Vortex beams with different topological numbers have different angular momentum, which contribute differently to the rotation rate of particles. The hollow rings of focused light in air with different topological numbers are shown in Fig. 4. In Figs. 4(a)–4(c), the hollow rings were generated by the MBSZP with topological numbers of 1, 2, and 3. The corresponding theoretical simulation results are shown in Figs. 4(d)–4(f). In a simulation, a Gaussian light beam was used as a light source, and the phase delay was π at the zone position of the MBSZP. The shape of the experimental light spot and the intensity distribution of the simulation show no qualitative difference. With increasing topological number, the ring's size also gradually increases in both experiment and simulation. The morphology of the quantitative characterization of the light spot is shown in Figs. 4(g)

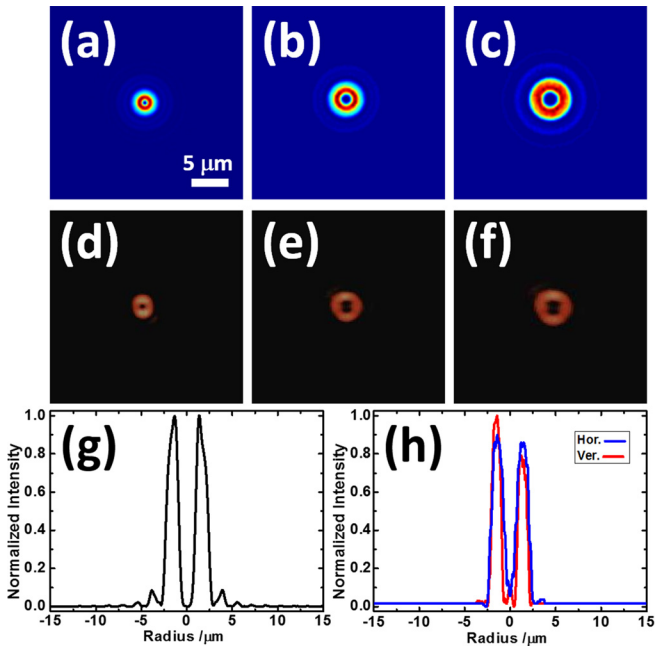

FIG. 4. Energy distribution of hollow rings with different topological numbers. (a)–(c) Theoretical simulation results. (d)–(f) Experimental results. (a) and (d), (b) and (e), and (c) and (f) Topological number are one, two, and three, respectively. (g) and (h) Theoretical and experimental normalized energy distribution in the cross section of hollow rings.

and 4(h), which were extracted from the energy distribution of light spot cross section. It clearly shows that the hollow ring diameters of simulation and experiment are 3.2 μm and 3.0 μm, which are in good agreement with each other. It is noteworthy that the mode purity of OV beams limited by the order of phase diffractive element.[18,36] The theoretical conversion efficiency of two level diffractive element is about 42%. The other energy diffuses on image plane, which reduces the mode purity. Fortunately, the problem can be solved by increasing the levels of MBSZP. The normalized energy distributions in horizontal and vertical directions are shown in Fig. 4(h) with red and blue lines. There is no obvious difference between the two curves, which shows that the hollow spot has a good symmetry.

The sizes of the light spots in the experiment and simulation are shown in Fig. 5. The topological numbers of the MBSZP are 1, 2, and 3. The diameters of the light spots in the experiment are 1.6 μm, 2.6 μm, 3.0 μm, respectively, and

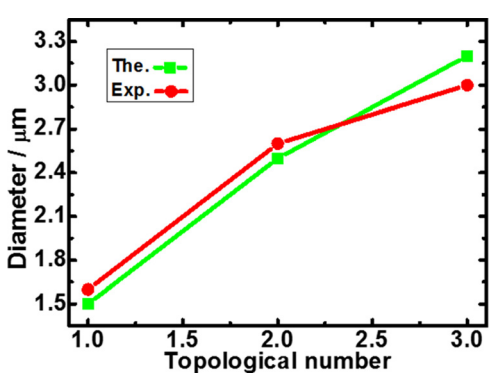

FIG. 5. Simulation and experimental results (in air) of hollow ring size with changing topological number.

1.5 μm, 2.5 μm, and 3.2 μm, respectively, in the simulation. The difference is less than 10%, which indicates that the MBSZP has the expected optical properties. The orbital angular momentum of the light beam also changes with the topological number. By changing the topological number of the MBSZP and incident laser power, the rotational speed of various sizes of particles can be controlled continuously.

In conclusion, we present an MBSZP, a micro OV beam generator. The MBSZP was buried under the surface of a crystal and demonstrated stable optical performance in various environments with different refractive indices. The focusing properties of the MBSZP with different topological numbers were investigated and showed a good agreement with the simulation results. Because the MBSZP is not sensitive to the refractive index of the external environment, it will have important applications in the manipulation of biological particles and coupling interfaces in complex liquid environments. In addition, the MBSZP will improve the integration and simplification of OV beam generation systems. It will fulfill important applications in optical manipulation, multistate information encoding, quantum communication, and computation.

The authors gratefully acknowledge the financial support from the National Natural Science Foundation of China under Grant Nos. 61137001, 91423102, 91323301, 61590930, and 61435005.

[1]L. Allen, M. W. Beijersbergen, R. J. C. Spreeuw, and J. P. Woerdman, Phys. Rev. A **45**, 8185–8189 (1992).
[2]H. H. Arnaut and G. A. Barbosa, Phys. Rev. Lett. **86**, 5209–5209 (2001).
[3]J. Wang, J. Y. Yang, I. M. Fazal, N. Ahmed, Y. Yan, H. Huang, Y. X. Ren, Y. Yue, S. Dolinar, M. Tur, and A. E. Willner, Nat. Photonics **6**, 488–496 (2012).
[4]T. Lei, M. Zhang, Y. R. Li, P. Jia, G. N. Liu, X. G. Xu, Z. H. Li, C. J. Min, J. Lin, C. Y. Yu, H. B. Niu, and X. C. Yuan, Light-Sci. Appl. **4**, e257 (2015).
[5]S. Franke-Arnold, L. Allen, and M. Padgett, Laser Photonics Rev. **2**, 299–313 (2008).
[6]J. E. Curtis and D. G. Grier, Phys. Rev. Lett. **90**, 133901 (2003).
[7]M. Padgett and R. Bowman, Nat. Photonics **5**, 343–348 (2011).
[8]M. E. J. Friese, J. Enger, H. Rubinsztein-Dunlop, and N. R. Heckenberg, Phys. Rev. A **54**, 1593–1596 (1996).
[9]G. Wright, M. J. Tucker, P. C. Morton, and S. E. Smith, Curr. Opin. Obstet. Gynecol. **10**, 221–226 (1998).
[10]D. G. Grier, Nature **424**, 810–816 (2003).
[11]Z. J. Yan and N. F. Scherer, J. Phys. Chem. Lett. **4**, 2937–2942 (2013).
[12]V. G. Shvedov, A. V. Rode, Y. V. Izdebskaya, A. S. Desyatnikov, W. Krolikowski, and Y. S. Kivshar, Phys. Rev. Lett. **105**, 118103 (2010).
[13]S. H. Tao, X. C. Yuan, J. Lin, X. Peng, and H. B. Niu, Opt. Express **13**, 7726–7731 (2005).
[14]K. Sueda, G. Miyaji, N. Miyanaga, and M. Nakatsuka, Opt. Express **12**, 3548–3553 (2004).
[15]E. Brasselet, M. Malinauskas, A. Zukauskas, and S. Juodkazis, Appl. Phys. Lett. **97**, 211108 (2010).
[16]N. R. Heckenberg, R. McDuff, C. P. Smith, and A. G. White, Opt. Lett. **17**, 221–223 (1992).
[17]J. Arlt, K. Dholakia, L. Allen, and M. J. Padgett, J. Mod. Opt. **45**, 1231–1237 (1998).
[18]G. Gibson, J. Courtial, M. J. Padgett, M. Vasnetsov, V. Pas'ko, S. M. Barnett, and S. Franke-Arnold, Opt. Express **12**, 5448–5456 (2004).
[19]M. J. Padgett and L. Allen, J. Opt. B: Quantum Semiclassical Opt. **4**, S17–S19 (2002).
[20]E. Karimi, B. Piccirillo, E. Nagali, L. Marrucci, and E. Santamato, Appl. Phys. Lett. **94**, 231124 (2009).
[21]M. Q. Mehmood, S. T. Mei, S. Hussain, K. Huang, S. Y. Siew, L. Zhang, T. H. Zhang, X. H. Ling, H. Liu, J. H. Teng, A. Danner, S. Zhang, and C. W. Qiu, Adv. Mater. **28**, 2533–2539 (2016).
[22]Y. M. Yang, W. Y. Wang, P. Moitra, I. I. Kravchenko, D. P. Briggs, and J. Valentine, Nano. Lett. **14**, 1394–1399 (2014).
[23]E. Karimi, S. A. Schulz, I. De Leon, H. Qassim, J. Upham, and R. W. Boyd, Light Sci. Appl. **3**, e167 (2014).
[24]X. L. Wang, J. Chen, Y. N. Li, J. P. Ding, C. S. Guo, and H. T. Wang, Phys. Rev. Lett. **106**, 189302 (2011).
[25]H. Lin and M. Gu, Appl. Phys. Lett. **102**, 084103 (2013).
[26]A. Balcytis, D. Hakobyan, M. Gabalis, A. Zukauskas, D. Urbonas, M. Malinauskas, R. Petruskevicius, E. Brasselet, and S. Juodkazis, Opt. Express **24**, 16988–16998 (2016).
[27]Z. F. Deng, Q. Yang, F. Chen, X. W. Meng, H. Bian, J. L. Yong, C. Shan, and X. Hou, Opt. Lett. **40**, 1928–1931 (2015).
[28]M. Malinauskas, A. Žukauskas, S. Hasegawa, Y. Hayasaki, V. Mizeikis, R. Buividas, and S. Juodkazis, Light Sci. Appl. **5**, e16133 (2016).
[29]Y. Liao, J. L. Ni, L. L. Qiao, M. Huang, Y. Bellouard, K. Sugioka, and Y. Cheng, Optica **2**, 329–334 (2015).
[30]Q. Sun, K. Ueno, H. Yu, A. Kubo, Y. Matsuo, and H. Misawa, Light Sci. Appl. **2**, e118 (2013).
[31]V. Mizeikis, V. Purlys, D. Paipulas, R. Buividas, and S. Juodkazis, J. Laser Micro/Nanoeng. **7**, 345–350 (2012).
[32]D. Paipulas, R. Buivydas, S. Juodkazis, and V. Mizeikis, J. Laser Micro. Nanoeng. **11**, 246–252 (2016).
[33]E. G. Gamaly, S. Juodkazis, V. Mizeikis, H. Misawa, A. V. Rode, and W. Krolikowski, Phys. Rev. B **81**, 054113 (2010).
[34]M. Ichikawa and K. Yoshikawa, Appl. Phys. Lett. **79**, 4598 (2001).
[35]S. B. Q. Tran, P. Marmottant, and P. Thibault, Appl. Phys. Lett. **101**, 114103 (2012).
[36]M. J. Strain, X. Cai, J. Wang, J. Zhu, D. B. Phillips, L. Chen, M. LopezGarcia, J. L. O'Brien, M. G. Thompson, M. Sorel, and S. Yu, Nat. Commun. **5**, 4856 (2014).